

A New Thermal Infrared Camera Calibration Approach Using Wireless MEMS Sensors

Peter Bajcsy and Sunayana Saha
National Center for Supercomputing Applications (NCSA)
University of Illinois at Urbana-Champaign, Illinois, USA
pbajcsy@ncsa.uiuc.edu, ssaha@uiuc.edu

ABSTRACT

This work presents a unique thermal infrared (IR) camera calibration technique using wireless “smart” micro electro-mechanical (MEMS) sensors. The word “smart” denotes capabilities of MEMS other than sensing, such as, computing and communication. We foresee the use of widely distributed and deeply embedded “smart” MEMS sensors as potential calibration gauges for spectral cameras, such as, thermal IR or visible spectrum cameras. Thus, the primary motivation of our presented work is to investigate the problem of spectral camera calibration in an indoor environment using the “smart” MEMS sensors. The main application of our work is in hazard-aware environments, or in any smart and intelligent spaces, where thermal cameras monitor thermal hazards with widely ranging temperatures and various temperatures require different actions to take place. We have investigated an optimal design of a calibration system with the MICA sensor hardware manufactured by Crossbow Inc. and programmed using TinyOS, and the thermal IR camera manufactured by Indigo System Corporation. We propose a robust calibration system design by maintaining two main objectives – minimizing the wireless loss of data transmitted by the sensors and maximizing the information content of the collected data. The first objective is fulfilled by experimentally determining an optimal sensor network that gives the least data losses. Maximization of information content is achieved by synchronizing, registering and calibrating acquired 2D images with precise point measurements obtained wirelessly from the MICA sensors.

Keywords: MEMS sensors, spectral camera, calibration, ad-hoc networks.

1 INTRODUCTION

Sensing devices are frequently used in smart spaces [8], [9],[10],[11] and include thermal IR cameras as well. Camera acquired images are often analyzed to build intelligent environments. While it has been known that one image is worth of one thousand words, the problem of extracting those words (or image content) automatically has not yet been solved.

The image content includes not only its spatial information, for example, object silhouettes, but also intensity or temperature profile information. In order to obtain temperature profile information from a thermal IR image and to discriminate hazardous temperatures from harmless temperatures, one has to convert the raw image values into engineering units, such as, degrees of Celsius or Fahrenheit or Kelvin. This conversion, also denoted as spectral calibration, is one out of many steps leading to image content understanding, so much needed in hazard aware spaces.

Our focus in this paper is on the calibration due to sensing mechanism that leads to unknown mapping between raw image pixel values and engineering units. The previous work on indoor spectral camera calibration problem can be classified into approaches based on (1) emitted (radiometric) or (2) reflected (photogrammetry based) energy/light using (a) black body or (b) reflectance gauges manually positioned in front of cameras and illuminated with specialized energy/light sources [12], [13]. We use the MEMS sensors (MICA motes) as our spectral gauges. The temperature sensors on the MICA motes provide us with point measurements that are then used to calibrate the thermal IR camera. In a case of outdoor thermal IR camera calibration, the approaches include additional considerations about atmospheric distortion, and passive and active type of sensing [13, Chapter 10], [14]. We do not take into account these issues. We foresee the use of widely distributed and deeply embedded “smart” micro electro-mechanical systems (MEMS) sensors as potential thermal IR calibration gauges for thermal IR cameras in future. Thus, the primary motivation of our presented work is to investigate the optimal design of a thermal IR camera calibration system in an indoor environment using the “smart” MEMS. To our knowledge, there has not been researched a thermal IR camera calibration system of this kind.

The development of miniaturized “smart” MEMS sensors, and particularly the MICA sensors, offers a great potential for obtaining billions of point measurements about any physical environment [6], [7]. The MICA sensor used in this work is one example of a “smart” MEMS sensor. The MICA hardware is manufactured by Crossbow Inc. [2] and

programmed using an open source operating system called TinyOS [4] that was developed by the University of California at Berkeley. The word “smart” is used to highlight the fact that MICA sensors consist of not only MEMS sensing electronics [3] but also some computational logic hardware and software with the capability of performing on-board computation [1]. The built-in support for wireless communication makes it possible to deploy MICA sensors in remote locations.

Our work on a new thermal IR calibration approach focuses on resolving any issues that occur, in general, during thermal IR camera calibration using any MICA thermal IR sensors. Our experimental test bed includes thermal infrared (IR) camera and the MICA sensors providing temperature and luminance readings. The thermal IR calibration problem is formulated as an optimization problem and solved by minimizing wireless information loss and maximizing information content. Although we have worked specifically with the thermal IR camera, our technique is general enough to be used for other kinds of spectral cameras. The novelty of our work lies in using ‘smart’ MEMS sensors as spectral gauges for camera calibration. Our method needs continuous data collection from the MEMS sensors and camera only for a short period of time, after which the data analysis is done on a dedicated PC.

This paper is organized as follows. First, we formulate the thermal IR calibration problem, propose our calibration approach and describe hardware components and a calibration procedure in Section 2. We focus then in Section 3 on meeting the two objectives, such as, minimization of wireless information loss and maximization of data information content. Our experimental results are presented in Section 4 and conclusions in Section 5.

2 THERMAL IR CALIBRATION

2.1 Formulation of Thermal IR Calibration Problem

The problem of thermal IR camera calibration using MICA sensors can be formulated as follows. Given a set of temporally changing, spatially local (point), temperature measurements obtained by MICA sensors and a set of temporally changing, two-dimensional (2D raster), thermal IR images viewing a subset of MICA temperature sensors, find the mapping between 2D image raw pixel values and their temperature values in engineering units. There are two additional considerations of the problem including (1) information loss due to wireless data communication between MICA sensors and the calibration station and (2) usefulness of raw measurements (information content) coming from

thermal IR camera and MICA temperature sensors. While the information loss is a function of MICA sensor network design, communication protocols and operational circumstances, the usefulness of raw image and MICA sensor measurements is futile without knowing temporal or spatial or thermal IR information, such as, the time stamp or location of temperature measurements in engineering units (degrees of Celsius or Kelvin and Fahrenheit). Thus, in addition to finding the mapping between 2D raster and point measurements in engineering units, the thermal IR calibration problem is constrained by minimization of wireless information loss and maximization of data information content.

2.2 Thermal IR Camera Calibration Approach

In general, a solution to the stated problem requires first a calibration of MICA temperature sensors with a thermal IR gauge, such as, a thermometer. We illustrated the calibration scheme by showing the three sensing devices, types of measurements obtained from these devices and their calibration dependencies in Figure 1. The thermal IR gauge provides measurements directly in engineering units.

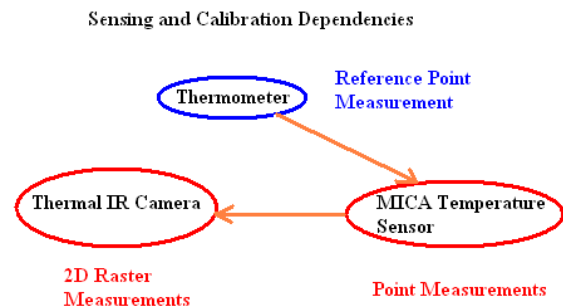


Figure 1. A schema of calibration dependencies given reference point (thermometer of thermal IR gauge), raster (thermal IR camera) and point (MICA temperature sensor) measurements.

According to the two arrows in Figure 1, there are two needed thermal IR calibration setups and they are shown in Figure 2. The two setups lead to finding (1) a transformation from MICA sensor raw measurements to the corresponding engineering units and (2) a transformation from thermal IR image raw values to the same engineering units. While establishing the first transformation is a manual process, building the second transformation can be fully automated. Furthermore, although the first transformation has to be established only once, it can be eliminated by using factory-calibrated sensors. In our thermal IR calibration approach, we consider the general case of un-calibrated point sensors, which is the case of MICA temperature sensors.

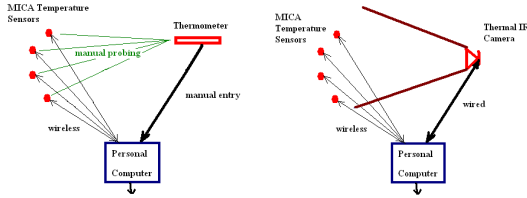


Figure 2. Two thermal IR calibration setups for calibrating MICA temperature sensor measurements (left) and thermal IR camera measurements (right).

2.3 Hardware Components of Thermal IR Calibration Setups

In our experiments, the temperature gauge is a regular thermometer used by chemists, measuring temperature directly in engineering units of degrees Celsius and providing temperature readings in the range $[-40^{\circ}\text{C}, 150^{\circ}\text{C}]$ with a reading uncertainty equal to $\pm 1^{\circ}\text{C}$. The thermal IR camera, the Omega model, is a long-wavelength (7.5-13.5 microns) uncooled microbolometer camera designed for infrared applications and manufactured by Indigo Systems Corporation, Goleta, CA. It is controlled via RS232 serial port and the analog NTSC video output is digitized using a Hauppauge WinTV board.

The MICA hardware is manufactured by Crossbow Inc [2] and it consists of (1) 4MHz Atmega 128L processor, (2) 128K bytes Flash, 4K bytes SRAM and 4K bytes of EEPROM, (3) 916MHz radio transceiver with a maximum data rate of 40Kbits/sec, (4) attached AA (2) battery pack and (5) plug-in sensor boards like the MTS101CA, attached through a 51-pin expansion connector. For more details, see [1]. The MTS101CA series sensor board [3] is attached to the MICA hardware and contains a precision thermistor and a light/photocell sensor. The EEPROM can be programmed using an open source operating system called TinyOS [4] that was developed by the University of California at Berkeley. TinyOS allows networking, power management and sensor measurements and is optimized for efficient computational, energy and storage usage. The key to TinyOS's functionality is the NesC (network-embedded-systems-C) compiler, which is used to compile TinyOS programs. NesC has a C like structure and provides several advantages such as interfaces, wire error detection, automatic document generation, and facilitation of significant code optimizations.

2.4 Thermal IR Calibration Procedure

Given the hardware components and thermal IR calibration setups described in previous sections, the proposed solution to the problem described in Section 2.1 can be described as follows. First, MICA sensors are programmed to sense and send temperature

readings over a certain time period. Second, during the same time period, temperature measurements are collected with a thermometer (a calibration gauge). Third, a calibration transformation is established for MICA temperature sensors as a combination of factory recommended formula and thermometer measurements. Fourth, MICA sensors are programmed to sense, track time based on an incremental counter, and send counter state together with temperature readings after receiving a RESET signal. One increment of a counter corresponds to 100 ms. Fifth, both thermal IR camera and MICA sensors are initiated to acquire data by broadcasting a RESET signal to MICA sensors and triggering thermal IR camera acquisition. Sixth, MICA sensors transmit every set (packet) of temperature measurements with the state of the internal counter to the base station attached to a personal computer (PC). In meantime, the thermal IR camera acquires data with the time stamp of the CPU clock counting from the RESET signal. Seventh, the MICA raw temperature measurements are received and transformed into degrees Celsius. Eights, MICA temperature sensor locations in the thermal IR image are identified, and statistics of the transformed MICA temperature measurements and the thermal IR image pixel values at the MICA sensor locations are related to form the final calibration transformation. In this step, if the entire scene viewed by a thermal IR camera is temperature homogeneous then MICA temperature sensor locations in the thermal IR image do not have to be identified and statistics of the thermal IR image can be computed over the entire image. The steps one through three are executed with the setup shown in Figure 2 (left) and the steps four through eight with the setup shown in Figure 2 (right). We believe that it provides a foundation for a new thermal IR calibration approach.

3 CALIBRATION OBJECTIVES

During the execution of the previously described thermal IR calibration procedure, we strive to meet two objectives, such as, minimization of wireless information loss and maximization of data information content. These two objectives are met by optimal MICA sensor network design (information loss aspect) and by sensor data packaging with temporal, spatial and thermal IR information (information content aspect). The process of meeting the two objectives is described next.

3.1 Minimization of Wireless Information Loss

The minimization of wireless information loss was achieved (1) by optimizing wireless data collection schemes and spatial arrangements of MICA sensors,

and (2) by experimental studies of wireless data loss as a function of a wireless distance from the receiving base station, number of active MICA sensors and number of other active wireless devices operating at different frequencies at the MICA communication time. In order to eliminate any extra problem complexity, we constrained our optimization effort to a single-hop MICA sensor networks. The information loss (IL) was calculated as a percentage of missing MICA sensor readings over the total number of expected MICA readings from all the active MICA sensors with expected 10 readings in each packet. The formula is provided below.

$$IL = \frac{\sum_i^{\text{numSensors}} \sum_j^{\text{numPackets}} \text{counter}(\text{packet}(i, j+1)) - (\text{counter}(i, \text{packet}(j)) + 10)}{\sum_i^{\text{numSensors}} \text{counter}(\text{packet}(i, \text{numPackets})) - \text{counter}(\text{packet}(i, 1))}$$

In terms of optimal wireless data collection schemes, we evaluated two different modes of operations, such as, Autosend and Query modes. In the Autosend mode, a sensor would send a packet to the base station as soon as it had 10 readings in its local array. Ideally, a sensor would transmit a packet for the temperature readings after every one-second (100 milliseconds/reading * 10 readings/packet = 1 second/packet). In the Query mode, a sensor still continuously senses the environment, but it does not send data as soon as it has the fixed number of readings in its local array. Instead, the base station queries each MICA sensor in a round robin fashion. When MICA receives a query message from the base station, it checks to see if a packet with 10 readings can be sent. If yes, it is sent immediately. Otherwise, it simply sets a local flag indicating that the base station query is pending. If 10 readings have been collected and the base station query is pending, then a packet with the readings is sent. However, if a MICA sensor does not have 10 readings at the query time then the packet is sent later and it may collide with another MICA's transmissions. We try to limit such a scenario by making the base station wait for a queried node's response for a finite amount of time, before it queries the next MICA sensor.

In terms of optimal MICA sensor spatial arrangements, we compared and evaluated (a) straight-line, (b) circular and (c) random MICA sensor placements. MICA sensors arranged in a 'straight-line' and within 10 to 15 inches from the base station and about 3 inches from each other. MICA sensors arranged in a 'circular' equidistant fashion around the base station with a radial distance of 10 inches between the base station and a MICA sensor. MICA sensors scattered in a 'random' fashion at a distance anywhere from 10 inches to 150 inches from the base station.

We evaluated wireless data loss as a function of MICA sensor distance from the base station by gradually increasing the distance to the maximum range of transmission (about 70 feet). Additional experimental studies were conducted to quantify the impacts of (a) the number of active MICA sensors from [1,7] operating at the same frequency and (b) transmission interference due to other active devices operating at similar and different frequencies, such as, cordless telephone, wireless LAN, wireless video and audio transmitters.

3.2 Maximization of Data Information Content

The maximization of information content was achieved by obtaining temporal, spatial and thermal IR information about each measurement.

The temporal information of MICA sensor measurements was obtained by introducing (1) a RESET signal to establish some reference time point and (2) a counter (timer) to track time. The temporal information of camera images was obtained during synchronization with the RESET signal and derived from an internal CPU clock rate of the main PC. While the counter (temporal) information for MICA measurements was sent inside of each wireless packet, the time stamp of each thermal IR camera image was part of the image metadata.

4 EXPERIMENTAL RESULTS

This section presents our findings about an optimal design of a thermal camera calibration system using MICA sensors. The optimal design is experimentally investigated with respect to the two objectives described in the previous section. All experiments were conducted in an indoor environment by sensing continuously the ambient temperature with MICA temperature sensors and recording values every 100 milliseconds. After every 100 milliseconds, the MICA sensor would obtain the raw temperature value through its ADC and store it in a local array. The local array size was fixed to hold only 10 readings. All experiments were confined to a relatively small laboratory, and therefore we used a 'single hop' MICA sensor network to relay data from a MICA sensor and the base station. The sensors were placed on a carpet floor such that they were in the field of view of thermal IR and visible spectrum cameras.

4.1 Minimization of Information Loss

The optimization results for wireless data collection schemes and spatial arrangements of MICA sensors can be summarized as follows. First, the percentage of readings lost in query mode is at least 10% higher than the readings lost in autosend mode (see Figure 3). As the number of nodes increases, the losses in

query mode shoot to about 50% while those in autosend stay around 15%. Thus, it is obvious that in terms of the number of readings lost, the autosend mode is far superior to the query mode. The explanation of this finding comes from the fact that these two simple modes depend either on slightly asynchronous transmission (autosend mode) to avoid packet collisions, or on fast and reliable data collection (query mode) to avoid waiting for data requests. It turns out that although all MICA sensors are synchronized in the beginning, the timers might be drifting and become out of sync later which improves the autosend mode performance. Furthermore, the medium access control (MAC) protocol, which is implemented in the lower levels of the TinyOS, can also be credited for slightly “out-of-sync” transmissions. On the other side, the existing network design variables, such as, increasing number of MICA sensors or larger travel distances or MICA failures, have a detrimental effect on the “query” mode performance.

Second, on average the most optimal spatial arrangements of MICA sensors were the equidistant circular arrangement. This finding can be explained by the theoretically desirable network configuration with equal distances between each MICA sensor and the base station in order to avoid dissimilar transmission time.

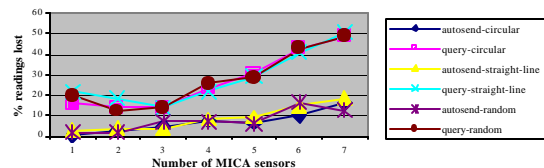


Figure 3. Percentage of readings lost in autosend and query modes.

The experimental results with multiple active MICA sensors and other wireless devices were obtained as follows. Due to the fact that the MICA sensors use a radio frequency of 916 MHz for wireless transmissions, another devices or MICA sensor networks in proximity could interfere with the transmission of our MICA sensors. We simulated such an independent MICA sensor network by placing some MICA sensors in the laboratory, which would broadcast meaningless data after every 150 milliseconds. Figure 4 shows how the data losses in our MICA sensor network increased as the number of “foreign” MICA sensors increased. The graph in Figure 4 clearly shows that the data loss is quite significant. The ‘foreign’ network is totally out-of-sync with our network and since its MICA sensors are transmitting at a much faster rate than our MICA sensor in autosend mode, our MICA sensor transmissions are likely suffering from more

collisions and hence lesser useful data are being received at the base station.

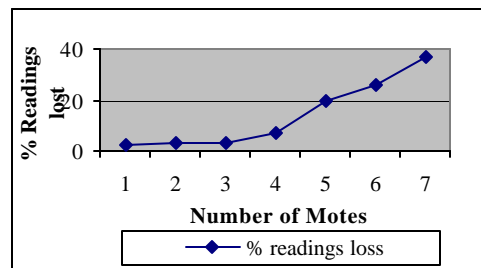


Figure 4. Percentage of readings lost as a function of number of motes in ‘other’ network.

In terms of other devices operating at other similar or very different frequencies, we experimented with (a) telephones and wireless video transmitters operating in the 900 MHz range, for example, a telephone (EnGenius SN920) and a video transmitter (accompanying CCTV-900 receivers), (b) wireless LAN (802.11b) operating at a frequency of 2.4 GHz and (c) wireless audio transmitters (audio-technica’s ATW-3110D) operating at frequencies between 655-680 MHz. In summary, the experiments in this category have shown that MICA transmissions are susceptible to interference from other devices that use the same frequency range for transmissions (100% loss). We have realized the MICA sensors are relatively low powered as compared to bigger devices like wireless cameras and telephones. Thus, in the presence of more powerful devices, a MICA sensor network is prone to total failure. In the presence of similarly powered devices, operating asynchronously with our MICA sensor network, the loss increases linearly as the number of MICA sensors in the ‘foreign’ network goes up.

4.2 Maximization of Information Content

First, we increased the stability of measurements coming from MICA sensors and thermal IR camera by temporal and spatial averaging before we seek temporal, spatial and thermal IR information associated with all measurements.

Second, we used Java’s Media Framework (JMF) to control the thermal IR camera image capture and obtain temporal information associated with camera measurements. JMF was used to start a new thread of execution (called ‘captureThread’) when the base station sends the ‘RESET’ message to the MICA sensors. ‘captureThread’ goes into an infinite loop of acquiring images from the thermal IR camera and saving them to disk. Each image is time stamped with the time when it was created since the start of ‘captureThread’. The temporal information for MICA sensor measurements was obtained according to our previous description.

In terms of the relative spatial position of MICA temperature sensors with respect to thermal IR camera, we co-registered visible spectrum and thermal IR images by using our set of software tools known as Image To Knowledge (I2K) [12]. We selected four points in the thermal IR and visible spectrum images, constructed an affine transformation matrix and transform one of the images. The four points were selected as the end points of two heated metallic wires in field of view of both cameras. These two wires appear as white lines in the thermal IR image in Figure 5 (right) and can be clearly seen in the visible spectrum image in Figure 5 (left).

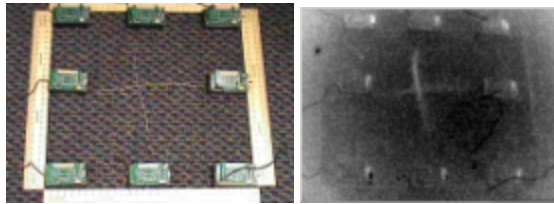


Figure 5. Visible spectrum image (left) used for MICA thermistor identification and the thermal IR image (right) after co-registration with the visible spectrum image.

Finally, we selected a linear function to model the MICA to pixel value mapping and constructed the final linear thermal IR calibration function using statistical averages and standard deviations according to the following formula:

$$T_{thermalIR}^{Calib}(C) = \frac{PixelVal - (\bar{\mu}_{thermalIR}^{Pixel} - \bar{s}_{thermalIR}^{Pixel})}{2\bar{s}_{thermalIR}^{Pixel}} 2\bar{s}_{MICA}^{Calib} + (\bar{\mu}_{MICA}^{Calib} - \bar{s}_{MICA}^{Calib})$$

The resulting calibrated thermal IR image is shown in Figure 6.

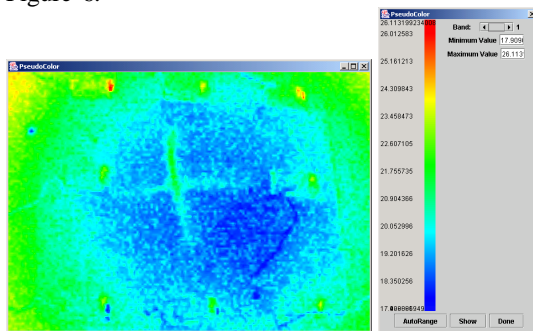


Figure 6. Registered pseudo-colored thermal IR image.

5 CONCLUSIONS

In this paper we presented a new thermal IR calibration approach using the MICA temperature sensors. We started by formulating the problem and outlining the calibration setups, hardware components and calibration procedure. Our novel

proposed calibration solution with MICA sensors was optimized by minimizing wireless information loss and maximizing information content. Our experimental results led to several conclusions about optimal sensor network design that contributed to our hazard aware space development. In our future work, we will focus on spectral calibration systems with MICA sensors that could be used for other than thermal IR cameras.

References

- [1] MICA sensor description, http://www.xbow.com/Products/Product_pdf_files/Wireless_pdf/MICA.pdf
- [2] Crossbow Inc. website <http://www.xbow.com>
- [3] Data sheet of the MTS101CA sensor board, http://www.xbow.com/Support/Support_pdf_files/MTS-MDA_Series_User_Manual_RevB.pdf
- [4] TinyOS website: <http://webs.cs.berkeley.edu/tos>
- [5] MICA: The Commercialization of Microsensor Motes <http://www.sensorsmag.com/articles/0402/40/>
- [6] Wang H., D. Estrin and L. Girod: "Preprocessing in a Tiered Sensor Network for Habitat Monitoring."
- [7] Mainwaing A., et al., "Wireless Sensor Networks for Habitat Monitoring", WSNA '02., Atlanta, Georgia, Sept. 28, 2002.
- [8] Vildjiounaite E., et al., "Smart Things in a Smart Home," the 5th Int. Conf. on Ubiquitous Computing, pp. 215-216, Seattle, WA, Oct. 2003.
- [9] Satyanarayanan, M. "Pervasive Computing: Vision and Challenges." IEEE Personal Communications, August 2001.
- [10] M. Weiser, "Some computer science issues in ubiquitous computing." Communications of the ACM, pages 75-84., July 1993.
- [11] Kidd, Cory D., et al., "The Aware Home: A Living Laboratory for Ubiquitous Computing Research," In the Proc. of the 2nd Int. Workshop on Cooperative Buildings (CoBuild), Pittsburg, October 1999.
- [12] Bajcsy P. et al., "Image To Knowledge", documentation at <http://alg.ncsa.uiuc.edu/tools/docs/i2k/manual/index.html>.
- [13] Campbell, J. B., *Introduction to Remote Sensing*, The Guilford Press, 1996.
- [14] Dinguirard, M. and P.N. Slater, 1999; "Calibration of Space-Multithermal IR Imaging Sensors: A Review"; *Remote Sensing of Environment*, 68(3): 194-205.
- [15] Saha S., and P. Bajcsy. "System Design Issues In Single-Hop Wireless Sensor Networks". In Proc. 2nd IASTED Int. Conf. on CIIT, pp. 743-748, Scottsdale, Arizona, November 2003.